Check for updates

Original Research Article

Exploring the Mechanism of Baicalein in Treating Oral Lichen Planus: A Network Pharmacology and Single-cell RNA Sequencing Analysis

Pharmacognosy Magazine
22(4) 1269–1280, 2026
© The Author(s) 2025
Article reuse guidelines:
in.sagepub.com/journals-permissions-india
DOI: 10.1177/09731296251387401
journals.sagepub.com/home/phm
Sage

Dan Zhou[1], Zehan Zhang[2], Zhilin Chen[2], Jianxing Zhang[1] and Chao Pei[1]

Abstract

Background: Oral lichen planus (OLP) is a prevalent chronic inflammatory oral mucosal disease with an uncertain pathogenesis and limited treatment options.
Objectives: This study aimed to systematically explore the underlying therapeutic mechanisms of baicalein in the treatment of OLP using network pharmacology and single-cell RNA sequencing analysis.
Materials and Methods: Baicalein target genes were sourced from the Comparative Toxicogenomics Database, SwissTargetPrediction, PharmMapper Server, and TargetNet. OLP gene expression data were retrieved from the GSE52130 dataset. Differentially expressed genes (DEGs), gene set enrichment analysis, and weighted gene co-expression network analysis (WGCNA) were performed to identify OLP-related targets by comparing DEGs with significant WGCNA modules. PPI networks were constructed using STRING and Cytoscape, and MCODE subgroup genes were assessed via *t*-tests and receiver operating characteristic (ROC) analysis. Immune infiltration analysis explored the immunomodulatory mechanisms. Single-cell RNA-seq identified cell types in erosive oral lichen planus (EOLP) and non-erosive oral lichen planus (NEOLP) groups and potential baicalein-sensitive cells. Molecular docking validated the target interactions.
Results: We identified 192 candidate targets of baicalein and 502 DEGs in OLP, with 409 OLP-related target genes emerging from the intersection of DEGs and WGCNA's pink and paleturquoise modules. PPI network and MCODE analysis refined these to 48 essential subgroup genes, which were further analyzed via Gene Ontology and Kyoto Encyclopedia of Genes and Genomes analyses, ultimately revealing 30 hub genes validated by *t*-test and ROC analysis. Immune infiltration analysis demonstrated baicalein's regulatory effects on $CD8^+$T cells and B cells, mitigating OLP-related immune dysregulation. Single-cell RNA sequencing highlighted divergent cell populations between EOLP and NEOLP groups, with monocytes emerging as key baicalein targets, supported by molecular docking confirming strong interactions with hub genes.
Conclusion: This study uncovered baicalein's multi-target mechanism in OLP, spanning immune regulation, metabolic reprogramming, and monocyte modulation, offering a rationale for preclinical validation.

Keywords

Baicalein, oral lichen planus, network pharmacology, single-cell RNA sequencing analysis, bioinformatics analysis

Received 24 January 2025; **revised** 06 July 2025; **accepted** 18 September 2025

Introduction

Oral lichen planus (OLP) is a prevalent chronic inflammatory disorder affecting the oral mucosa (Ahn et al., 2020). Although OLP typically arises on the buccal mucosa, lesions may additionally involve the gingiva, tongue, lips, or palate (Park et al., 2018). OLP affects roughly 0.5%–2% of adults, with a female-to-male ratio of about 2–3:1 (Li et al., 2019).

OLP could progress to oral squamous cell carcinoma, underscoring the urgency for effective treatment strategies (Peng et al., 2017). However, the molecular mechanism underlying OLP remains unclear, leading to a lack of targeted treatment (Ding et al., 2017). Currently, corticosteroids are the primary choice for OLP lesions. In addition, retinoic acid, vitamin A analogs, and

Dan Zhou and Zehan Zhang contributed equally to this study.
[1]Department of Stomatology, Zhejiang Hospital, Hangzhou, Zhejiang, China
[2]School of Traditional Chinese Medicine, Beijing University of Chinese Medicine, Beijing, China

Corresponding author:
Chao Pei, Department of Stomatology, Zhejiang Hospital, Hangzhou, Zhejiang 310013, China.
E-mail: pc1224pc@163.com

Creative Commons Non Commercial CC BY-NC: This article is distributed under the terms of the Creative Commons Attribution-NonCommercial 4.0 License (http://www.creativecommons.org/licenses/by-nc/4.0/) which permits non-Commercial use, reproduction and distribution of the work without further permission provided the original work is attributed as specified on the SAGE and Open Access pages (https://us.sagepub.com/en-us/nam/open-access-at-sage).

photodynamic therapy are commonly used in the clinical treatment of OLP. While these could lead to side effects such as skin thinning, brittleness, and permanent stripes, some of which persist a long time after treatment cessation (Choi et al., 2022). This has spurred researchers to explore traditional Chinese medicine and its monomer compounds, aiming to discover more effective treatments with fewer side effects.

Baicalein is the bioactive component of *Scutellaria baicalensis* (Markowski et al., 2023). Baicalein features good anti-inflammatory, anti-apoptosis, and anti-tumor activities, which have been widely used in cardiovascular diseases, stroke, diabetic nephropathy, cancer, and other diseases. Current first-line OLP treatments primarily target immune suppression through single-pathway interventions. However, their long-term use is limited by side effects. In comparison, baicalein exhibits a polypharmacological profile that simultaneously addresses multiple pathological hallmarks of OLP (Guan et al., 2023; Lee et al., 2022; Peng et al., 2023). Baicalein has also been widely applied in oral diseases. Moreover, several studies have indicated its significant inhibitory effect on oral squamous cell carcinoma, with studies showing it inhibits IL-6/STAT3 signaling and modulates the NF-κB pathway (Gao et al., 2020; Li et al., 2017). Unfortunately, despite these promising findings, a systematic analysis of baicalein's mechanism in treating OLP is still lacking.

Network analysis is an effective approach for elucidating the pharmacological effects and regulatory pathways of drugs concerning disease treatment. This method allows the identification of interaction patterns among the active components, targets, and potential action mechanisms of herbs (Li & Zhang, 2013). Complementing this approach, single-cell RNA sequencing is a valuable method for clustering and annotating dispersed cells within samples, facilitating the prediction of drug sensitivity across cells originating from diverse sources, which holds significant promise in advancing the development of innovative pharmaceutical interventions (Zheng et al., 2023). Molecular docking, a core *in silico* tool, pinpoints how tightly and in what pose bioactive ligands engage their targets (Huang et al., 2023). In this study, we integrated network pharmacology analysis and single-cell RNA sequencing analysis to unravel baicalein's potential mechanism in treating OLP. Docking simulations were then run to map how baicalein exerts its therapeutic effect. The flowchart illustrates the details of the study design (Figure 1).

Materials and Methods

Target Identification of Baicalein

Potential targets of baicalein were identified using multiple databases, including the SwissTargetPrediction database (https://www.swisstargetprediction.ch/), Comparative Toxicogenomics Database (CTD; https://ctdbase.org/), TargetNet database (https://targetnet.scbdd.com/), and PharmMapper Server (http://www.lilab-ecust.cn/pharmmapper/). In the CTD database and PharmMapper Server, we screened higher-than-average targets

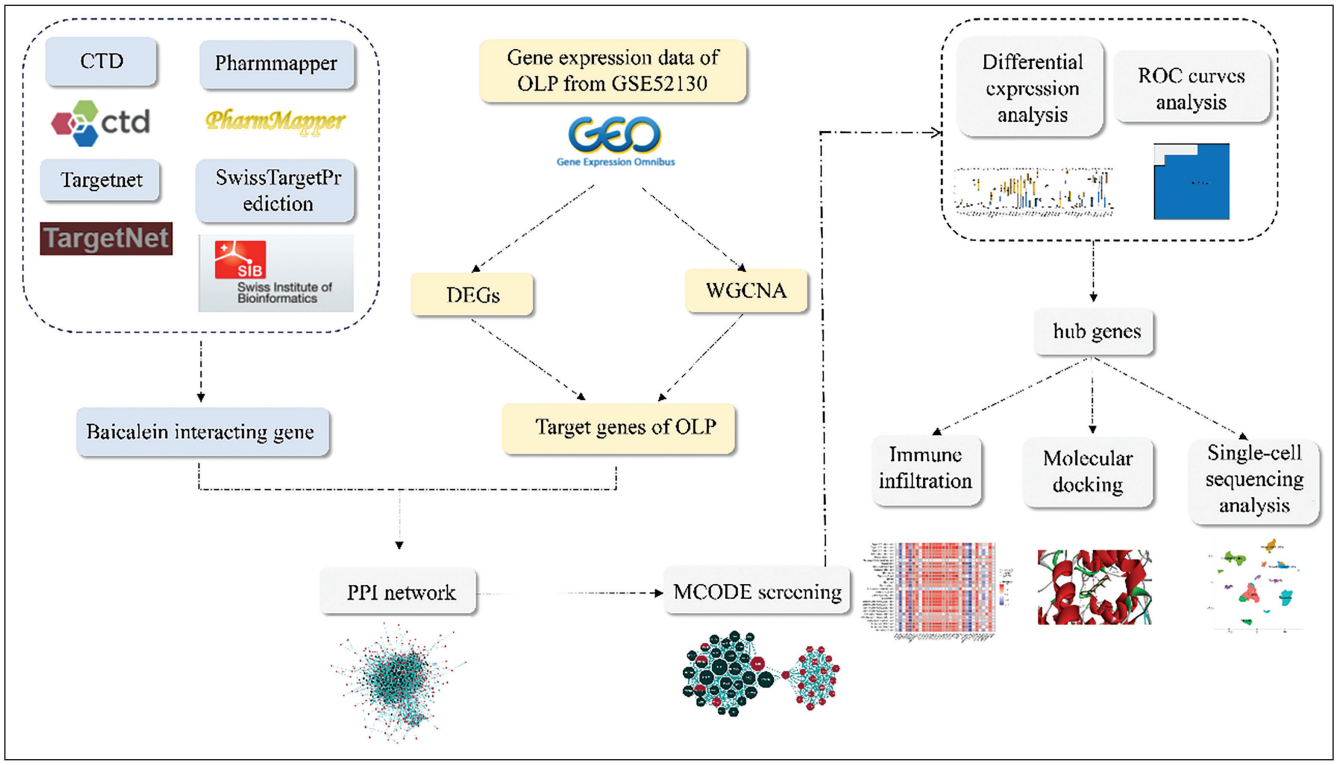


Figure 1. A Flowchart of Our Study Design.

according to their interaction count and Norm Fit, respectively. Finally, the potential targets of baicalein were obtained by combining the results from these databases. The UniProt database (https://www.uniprot.org/uploadlists/) was used to normalize the potential targets associated with baicalein (The UniProt Consortium, 2018). Gene Ontology (GO) analysis and Kyoto Encyclopedia of Genes and Genomes (KEGG) pathway analysis were conducted using the Bioconductor packages in R software to analyze the baicalein-related targets. Data visualization was performed using the ggplot2 tool in R software (version 4.2.0).

Identification of Differentially Expressed Genes (DEGs) in OLP

Gene expression profiling and corresponding clinical information of OLP were obtained from the Gene Expression Omnibus (GEO) database (https://www.ncbi.nlm.nih.gov/geo/). The GSE52130 set supplied 14 specimens: seven OLP and seven matched normal oral epithelia. The gene expression matrix was first normalized and integrated. Then the DEGs between OLP and controls were identified using the R package "limma (version 4.2)" with the Benjamini–Hochberg method for p value adjustment. DEGs were defined based on $|\log2 \text{ (fold change)}| > 1$ and $p < .05$. Gene set enrichment analysis (GSEA) was conducted using GSEA software (version 3.0, http://www.gsea-msigdb.org/gsea/index.jsp) to identify biological pathways and processes implicated in OLP pathogenesis.

Weighted Gene Co-expression Network Analysis

Weighted gene co-expression network analysis (WGCNA) was performed for scale-free network topology analysis. The WGCNA process mainly included the following steps (Zhao et al., 2022): The process begins by defining the similarity matrix and transforming it into an adjacencies matrix using a selected weight coefficient β. This matrix is then converted into a topological overlap matrix (TOM). A hierarchical clustering tree is obtained by performing hierarchical clustering on the TOM-based dissimilarity measure, from which modules are identified using the dynamic tree cutting method. Finally, the eigengene is calculated for each resulting module, and the Pearson correlation coefficient between MEs of each module was calculated (Guillotin et al., 2021).

Protein–Protein Interaction Network Construction

The protein–protein interaction (PPI) network was constructed using the STRING database (https://string-db.org/), where nodes and edges represent proteins and their high-confidence interactions, respectively. The resulting network was visualized with Cytoscape software (version 3.7.1). Furthermore, densely connected regions within this network were identified using the molecular complex detection (MCODE) algorithm.

Differential Expression of Essential Subnetwork Genes in OLP and Normal Tissues

Receiver operating characteristic (ROC) curves were plotted to assess the prognostic impact of essential MCODE subnetwork genes on OLP using the area under the curve (AUC). Genes with AUC > 0.75 were considered to have excellent robustness for OLP diagnosis. Genes satisfying the t-test and AUC > 0.75 were identified as core subnetwork genes.

Immune Infiltration Evaluation

Single sample gene set enrichment analysis (ssGSEA) was used for the algorithm of immune infiltration. Correlation analysis using the Spearman method was performed to determine the relationship between the core subnetwork gene and 28 types of immune cells. A significant correlation between core subnetwork gene expression and immune cells was established when $p < .05$. The results were visualized as a heatmap.

Single-Cell RNA Sequencing Data Analysis and Identification of Core Subnetwork Genes

The original single-cell RNA-Seq dataset (GSE211630) used in our analysis was obtained from the GEO database. The dataset comprised biopsies from five patients with OLP. Two patients with erosive lesions in biopsies were categorized as the erosive oral lichen planus (EOLP) group, while the remaining three patients without erosive lesions in their biopsies were classified as the non-erosive oral lichen planus (NEOLP) group. Tissues were extracted from the patients and analyzed using expression profiling microarrays on the Illumina NovaSeq 6000 platform. The Seurat R package (version 4.2.0) was used for preprocessing the raw dataset to ensure the data quality. Cells were retained only if they met the following criteria: nFeature_RNA > 200 and < 10,000, percent.mt < 20%, and percent.rb < 20%. The "JackStraw" function was used to determine the Principal Component value. We also built a KNN graph based on Euclidean distance in the reduced-dimensional principal component analysis (PCA) space and performed cell clustering at set resolutions. Cell visualization was achieved through t-SNE plots. Following this, SingleR was used for automated cell-type annotation. The final step involved analyzing the correlation between core subnetwork genes and the various cell types, thereby revealing the genes' distribution patterns.

Molecular Docking

In this study, proteins corresponding to the core subnetwork genes served as macromolecular protein receptors, while baicalein acted as the small molecular ligand.

The core subnetwork genes were mapped to their corresponding human protein sequences via the UniProt database. These sequences were then submitted to the Swiss-Model

server for homology modeling, yielding the three-dimensional structure of the macromolecular protein. For the ligand, the 3D structure of baicalein was acquired from the PubChem database. Molecular docking, including pocket identification, was performed using CB-Dock2, with the resulting ligand-receptor interactions validated by calculating the free binding energy.

Results

Target Genes of Baicalein

From the databases, we identified and retrieved 192 target genes associated with baicalein (Supplementary Figure 1A; Supplementary Table 1). Subsequently, GO functional enrichment and KEGG pathway enrichment analyses were performed (Supplementary Figure 1B–D; Supplementary Tables 2–3). GO term enrichment analysis identified significant terms across all three categories. The biological processes were predominantly related to responses to xenobiotic and metal ion stimuli, as well as a spectrum of metabolic processes. Cellular component analysis revealed enrichment in the membrane raft, the membrane microdomain, and the vesicle lumen. Meanwhile, molecular function was characterized by significant enrichment in nuclear receptor activity, ligand-activated transcription factor activity, and a specific oxidoreductase activity. KEGG analysis revealed enrichment mainly in the pathways related to cancer, endocrine resistance, nitrogen metabolism, arachidonic acid metabolism, and the relaxin signaling pathway.

DEGs of OLP

Following normalization (Supplementary Figure 2A,B), 502 genes were screened out as DEGs between OLP samples and normal tissue in the GSE52130 dataset (Supplementary Table 4). Among these, 211 genes were upregulated, and 291 genes were downregulated. The genes with |log2 (fold change)| > 3 and $p < .01$ were marked in the volcano plot (Supplementary Figure 2C). GSEA pathway enrichment analysis was conducted between the OLP and control groups (Supplementary Figure 2D). The results showed that ascorbate and aldarate metabolism, butanoate metabolism, DNA replication, Lysine degradation, and Phenylalanine metabolism were significantly upregulated in OLP (Supplementary Figure 2E). Conversely, allograft rejection, asthma, graft-versus-host disease, malaria, and type I diabetes mellitus were significantly downregulated in OLP (Supplementary Figure 2F). These dysregulated pathways suggested profound metabolic and immune alterations in OLP pathogenesis.

WGCNA

To enhance the accuracy of WGCNA, low-quality transcripts (mean FPKM < 1 across all samples) were filtered out, and we finally obtained 14 samples and 34589 genes from the GSE52130 dataset for subsequent analysis (Yang et al., 2023). After confirming no significant outliers, we determined the optimal soft-thresholding power ($\beta = 5$) using the pickSoftThreshold function, ensuring the network achieved a scale-free topology fit index ($R^2 > 0.85$, Figure 2A) (Fang et al., 2022). Dynamic tree cutting identified 58 distinct co-expression modules, among which two exhibited significant associations with OLP. By correlating the gene co-expression modules with clinical characteristics, we identified two modules significantly correlated with OLP: the pink module (Cor = −0.87, $p = 6e^{-05}$) was significantly downregulated in the OLP group and upregulated in the healthy control group, while the paleturquoise module (Cor = 0.81, $p = 6e^{-04}$) exhibited the opposite expression pattern (Figure 2B, C). Scatter plots also showed a strong correlation between gene significance and module membership in the pink and paleturquoise modules (pink: Cor = 0.83, $p = 1e^{-200}$; blue: Cor = 0.78, $p = 5.2e^{-143}$), indicating that genes central to these modules were strongly linked to OLP phenotype (Figure 2D,E; Supplementary Table 5).

PPI Network Construction and Essential Subgroup Genes Identification

To elucidate how baicalein might interact with these disease-associated targets, we constructed a PPI network integrating both OLP-related genes and baicalein targets. A total of 409 OLP-related target genes were identified by intersecting the genes in the pink and paleturquoise modules of WGCNA with DEGs (Figure 3A; Supplementary Table 6). Furthermore, 409 OLP-related target genes and 192 baicalein-related target genes were imported into the STRING online database for PPI network construction (nine genes were OLP and baicalein common genes) (Figure 3B; Supplementary Table 7). After removing aberrant proteins, a PPI network with 397 proteins was ultimately obtained (Figure 3C). Cytoscape software was used for PPI network visualization. The nodes from different sources were marked with different colors (red nodes representing OLP-related targets, and green nodes representing baicalein-related targets). A network diagram visualized the node interconnections, with red-green nodes denoting baicalein's direct potential targets and green lines indicating its indirect links to OLP-related genes. The MCODE plug-in identified the most significant subgroup in the PPI network (MCODE score = 22.766), a robust cluster of 48 nodes and 535 edges (Figure 3D), which were defined as essential subgroup genes (Supplementary Table 8).

Analysis of MCODE Essential Subgroup Genes

The MCODE essential subgroup genes showed significant enrichment in biological processes related to skin development and epidermal differentiation, including keratinization and keratinocyte differentiation. Molecular function analysis

Table 1. Molecular Docking Results Between Baicalein and Hub Targets.

Target	Binding Energy (kJ mol^{-1})	Cavity volume (Å3)	Center (x, y, z)	Docking size (x, y, z)
APP	−7.8	2792	5, 8, 7	27, 20, 28
CASP9	−8.1	3888	29, 51, 16	31, 20, 20
CCND1	−6.4	180	−6, 23, 38	20, 20, 20
CDSN	−7.6	2657	−1, 1, −3	20, 20, 28
EGFR	−8.5	2285	25, 37, 36	32, 20, 30
HMOX1	−8.4	1402	−24, −22, 168	20, 20, 20
HSP90AA1	−7.8	705	40, –48, 65	20, 20, 20
IL1B	−6.6	151	19, 3, 84	20, 20, 20
LCE1B	−5.2	1	−3, 6, −3	20, 20, 20
LCE1C	−4.9	13	0, 6, −6	20, 20, 20
LCE2A	−5.4	46	7, 8, 15	20, 20, 20
LCE2B	−4.3	86	−21, −14, 29	20, 20, 20
LCE2C	−4.3	96	−21, −15, 28	20, 20, 20
LCE2D	−5.1	32	−1, 6, −2	20, 20, 20
LCE3A	−5.1	3	−23, −10, 15	20, 20, 20
LCE3D	−4.9	3	−19, 0, −2	20, 20, 20
LCE3E	−4.8	6	19, 21, −2	20, 20, 20
LCE6A	−4.5	11	28, −8, −17	20, 20, 20
LOR	−5.3	6	−22, −39, −19	20, 20, 20
MMP2	−8.8	467	75, 107, 168	20, 20, 20
PI3	−7.3	119	5, 16, 52	20, 20, 20
PPARA	−8.5	2319	35, 37, 41	20, 20, 27
PPARGC1A	−7.2	626	−14, 56, 34	20, 20, 20
PTGS2	−9.5	4431	14, 49, 65	26, 29, 29
RPTN	−8.1	17512	−16, 11, 14	35, 35, 35
SPRR1B	−4.7	4	−81, −3, 53	20, 20, 20
SPRR2B	−5.3	13	58, −4, −46	20, 20, 20
SPRR2E	−5.2	17	61, −5, −39	20, 20, 20
SPRR2G	−5.0	16	−64, 7, 53	20, 20, 20
SRC	−7.4	293	47, 7, 25	20, 20, 20

highlighted roles in transcription factor binding and phosphatase binding (Figure 3E; Supplementary Table 9). KEGG pathway analysis further identified their involvement in hormone-related signaling pathways such as estrogen, prolactin, and relaxin (Figure 3F,G; Supplementary Table 10). To evaluate their clinical relevance, we assessed the differential expression of these genes in the GSE52130 dataset, identifying 30 genes that were significantly altered in OLP. These were established as hub genes based on their diagnostic performance in ROC curve analysis (Supplementary Figure 3A,B; Supplementary Table 11).

Immune infiltration analysis suggested significant differences in the distribution of 28 immune cell types among the 14 samples (Figure 4A). The violin plot revealed that gamma delta T cell, plasmacytoid dendritic cell, and memory B cell were significantly upregulated in OLP samples, while central memory CD8$^+$ T cell was downregulated in OLP samples (Figure 4B). The correlation heatmap revealed that the 30 hub genes were strongly correlated with various infiltrating immune cells, including Type 17 T helper cells, Neutrophils, Monocytes, and multiple B and T cell subtypes, indicating their primary involvement in immune regulation. Among these, CASP9, EGFR, PI3, and PPARGC1A appeared to be particularly important for regulating immune function in OLP (Figure 4C).

Single-cell RNA Sequencing Data Analysis

We found a strong positive correlation between nCount_RNA and nFeature_RNA in both the EOLP and NEOLP groups

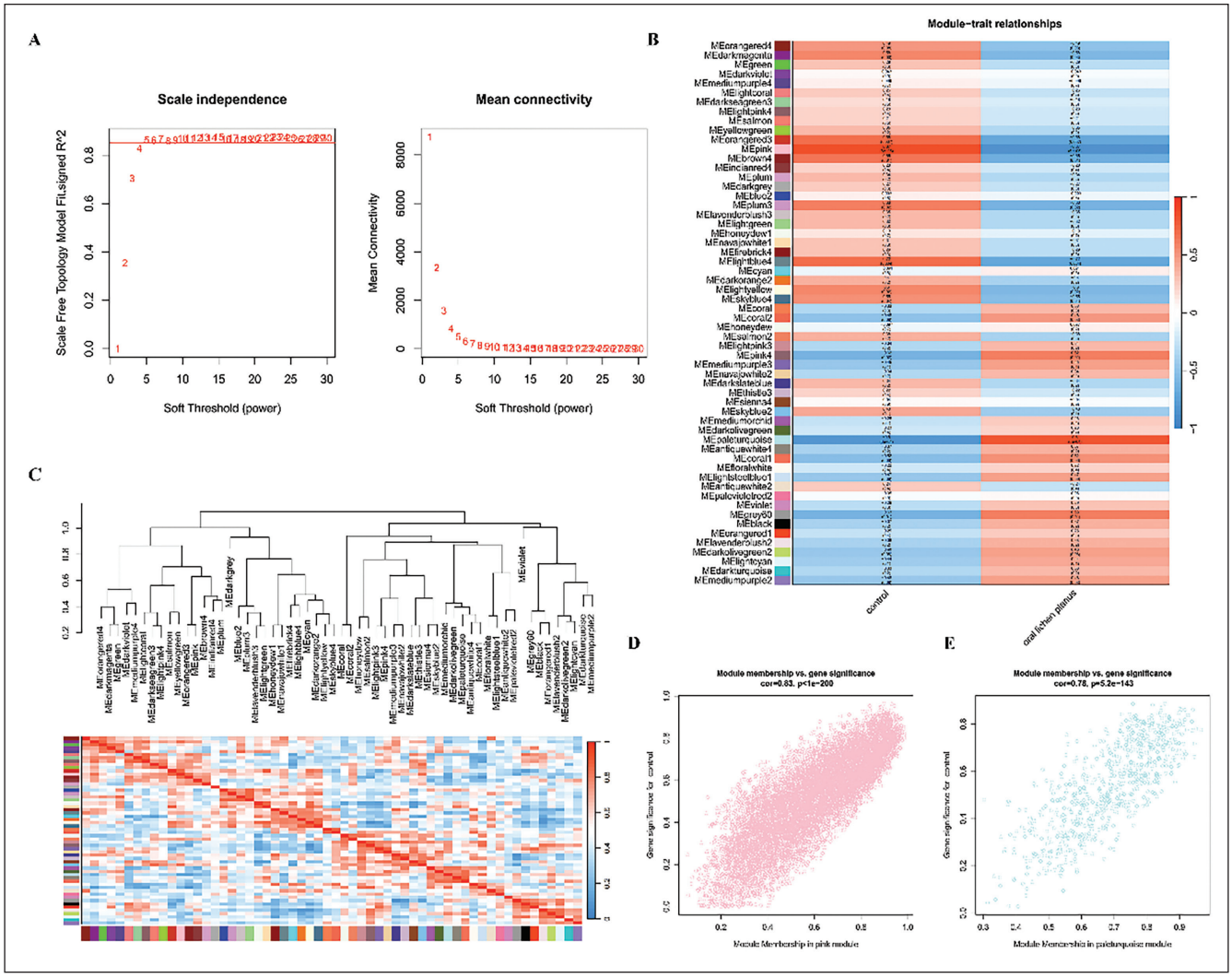


Figure 2. Weighted Gene Co-expression Network Analysis (WGCNA) Enrichment Analysis. (A) Selection of Soft Threshold Power. (B, C) Module Connections with Oral Lichen Planus (OLP). (D) Pink Module Genes and OLP. (E) Paleturquoise Module Genes and OLP.

(Supplementary Figure 4A–D). Using the Seurat package, we applied the percent feature set function to ensure that the measured nFeature_RNA was between 200 and 10,000, and both percent.mt and percent.rb were below 20% (Supplementary Figure 4C,D). The cluster tree was scaled to a resolution of 1.5 (Supplementary Figure 4I,G) in both NEOLP and EOLP samples, leading to the division of all samples into 20 cell subgroups (Supplementary Figure 4K,L). Marker genes for each cell subgroup were identified, and cells were visualized in low-dimensional space following dimensionality reduction using UMAP plots, which also aid in clustering and annotation (Figure 5B,F). SingleR-based annotation revealed the cellular composition: the EOLP group comprised T cells, tissue stem cells, endothelial cells, NK cells, monocytes, smooth muscle cells, B cells, and neutrophils, whereas the NEOLP group contained T cells, smooth muscle cells, monocytes, endothelial cells, tissue stem cells, B cells, epithelial cells, keratinocytes, DCs, and NK cells (Figure 5C,G).

Among the 30 hub genes, differential expression was observed in five genes from EOLP samples and nine from NEOLP samples, as visualized in the heatmaps (Figure 5A,B). The cellular expression distribution, scored by AUCell, further differentiated the two groups: hub genes were mainly expressed in monocytes in EOLP (Figure 5D), in contrast to smooth muscle cells in NEOLP (Figure 5H).

Molecular Docking Results

We performed preliminary verification of the binding ability of 30 hub genes to baicalein through molecular docking experiments. Table 1 demonstrates that 22 docking experiments resulted in binding free energies less than −5 kJ mol−1, indicating that there is a strong binding ability between hub

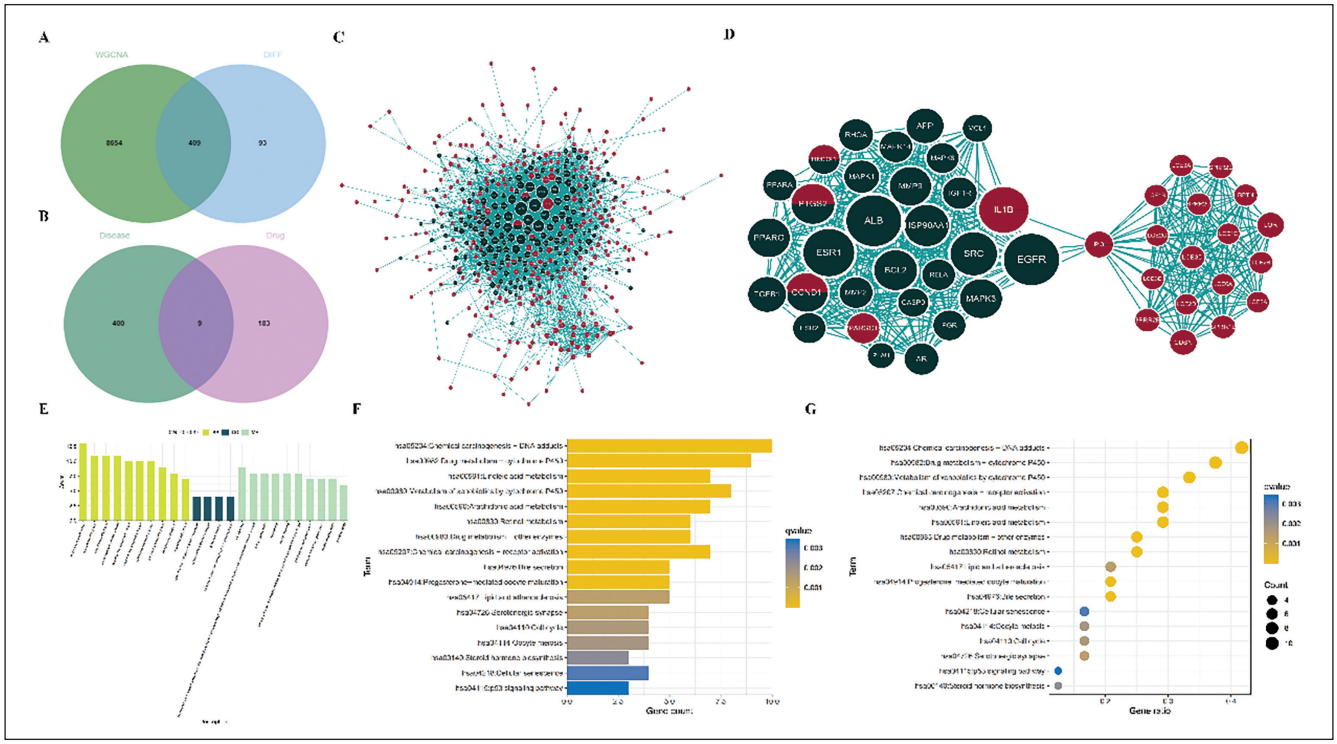


Figure 3. Protein–Protein Interaction (PPI) Network Construction and Essential Subgroup Genes Identification. (A) Overlapping Genes. (B) Disease and Drug Targets. (C) PPI Network. (D) Important Gene Subgroup. (E) Function of Highest-scoring Molecular Complex Detection (MCODE) Subgroup Feature Genes. (F, G) Pathways of Highest-scoring MCODE Subgroup Feature Genes.

genes and baicalein. Notably, PTGS2, MMP2, EGFR, PPARA, HMOX1, CASP9, RPTN, APP, HSP90AA1, CDSN, SRC, PI3, and PPARGC1A all exhibited excellent binding ability with baicalein (binding free energy > 7.0 kJ mol−1). We selected the ligand with the lowest binding free energy to the receptor, and then visualized the three receptor-ligand interactions with the lowest binding free energies using Discovery Studio software. As shown in Supplementary Figure 5A–C, these visualizations provide a clear representation of receptor-ligand interactions, amino acid residues, and protein pockets. The analysis identified key residues for baicalein binding, such as GLU525, GLN480, and ASP622 in MMP2. Notably, short hydrogen bonds (2.02 Å, 2.87 Å) with ASP622, along with Pi-Alkyl interactions (e.g., with LYS40, ALA38, and LEU17 in EGFR), were observed. These specific interactions are critical for stabilizing the ligand within the protein pockets. In summary, the molecular docking results demonstrated that baicalein can directly exert therapeutic effects on a large number of OLP targets. These findings provide compelling evidence for the therapeutic potential of baicalein in OLP.

Discussion

In this study, we found that ascorbate and aldarate metabolism, butanoate metabolism, DNA replication, lysine degradation, and phenylalanine metabolism were closely related to the pathogenesis of OLP *via* GSEA analysis. A clinical investigation has highlighted a deficiency in ascorbic acid among OLP patients (Nicolae et al., 2017). DNA replication anomalies have been frequently observed in OLP patients (Sperandio et al., 2016). Additionally, the DNA mismatch repair protein HMSH2 has emerged as a potential biomarker for assessing cancer risk in OLP patients (Li et al., 2015). Amino acids have proven to be one of the useful tools for detecting biomarkers of various oral diseases and monitoring disease progression (Hyvärinen et al., 2023). However, previous research has not linked lysine and phenylalanine metabolic processes to OLP's pathological mechanisms; thus, further research is warranted. The monomers of traditional Chinese medicine exhibit multi-target regulation, which enables them to exert therapeutic effects on complex diseases from various perspectives (Chen et al., 2020).

The incidence of OLP is affected by serum estrogen levels, which makes OLP more common in women (Gholizadeh et al., 2021). It has been observed that estradiol, a significant estrogen, reinforces the physical barrier of the oral epithelium by acting on nuclear estrogen receptors and increasing the expression of tight junction proteins. (Choi et al., 2018). Serum IL-17 levels were significantly elevated in patients with EOLP compared to those with NE OLP and healthy subjects (Pouralibaba et al., 2013). Baicalein can regulate Th17/Treg cell differentiation to reduce the level of

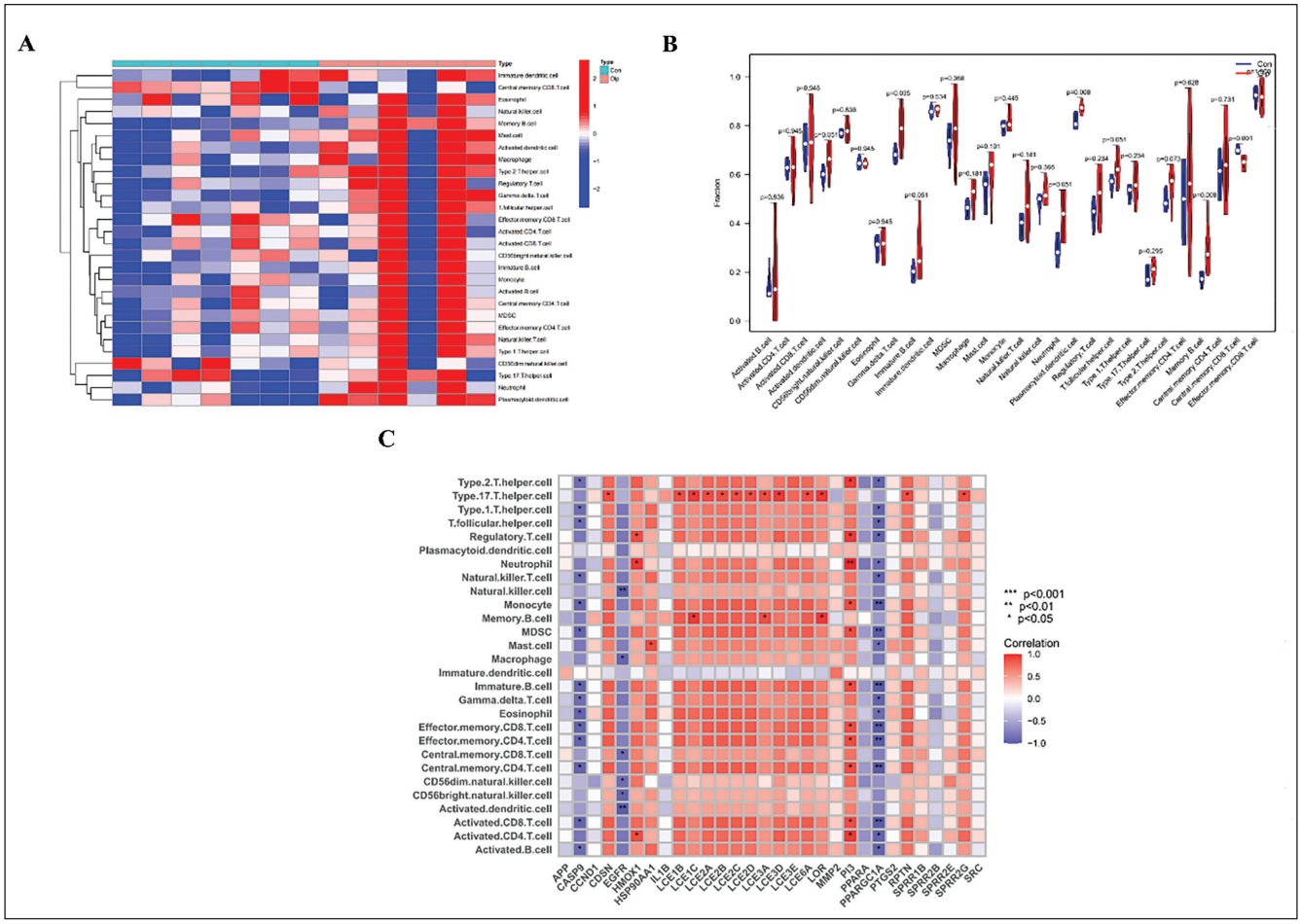


Figure 4. Immune Infiltration Evaluation Through Single Sample Gene Set Enrichment Analysis (ssGSEA) Algorithm. (A) The Heatmap Shows the Difference in Immune Infiltration Between Control Group and Oral Lichen Planus (OLP) Group. Red Indicates Immune Cell Infiltration, and Blue Indicates Suppressed Immune Cells. (B) The Violin Plot Shows the Difference Between Various Immune Cell Types in Control Group and OLP Group. (C) Relationship Between Hub Genes and Immune Cells. Red Indicates a Negative Correlation, and Blue Indicates a Positive Correlation. Deeper Colors Indicate Stronger Correlation. Correlation Significance is Indicated by Asterisks (*$p < .05$, **$p < .01$, ***$p < .001$).

proinflammatory cytokine IL-17, thereby inhibiting inflammation (Liu et al., 2020). Prolactin is an immunomodulatory hormone that promotes the occurrence of lichen planus and serves as a biomarker of disease activity in lichen planus (Gupta et al., 2017). However, direct evidence linking baicalein to prolactin pathway modulation remains absent in the literature. This finding, therefore, represents a testable hypothesis rather than an established mechanism.

Baicalein exhibits the highest affinity with PTGS2, MMP2, and EGFR, implying that these molecular entities are the primary candidates for baicalein's intervention in OLP. PTGS2 plays a central role as one of the main enzymes driving inflammation (He et al., 2022). PTGS2 levels in buccal mucosa biopsy tissues were approximately four-fold higher in OLP patients than in controls (Rankin et al., 2020). Significant upregulation of MMP-2 expression was observed in tissue samples of patients with OLP (Wang et al., 2016). The upregulation of MMP-2 promotes abnormal keratinocyte proliferation, thereby contributing to the pathogenesis of OLP (Wang et al., 2016). EGFR is one of the key regulatory proteins in the growth of epidermal cells (Bao et al., 2022). Overexpression of EGFR has been reported in the clinical samples of OLP, which may contribute to the carcinogenesis of this disease (Kumagai et al., 2010). Numerous pharmacological investigations have substantiated that baicalein can exert direct or indirect effects on PTGS2, MMP2, and EGFR across various pathological conditions. Thus, we identify PTGS2, MMP2, and EGFR as the core targets underlying baicalein's efficacy in treating OLP.

The pathogenesis of OLP is strongly associated with immune dysregulation (Zhong et al., 2020). Immune infiltration analysis revealed significant alterations in gamma

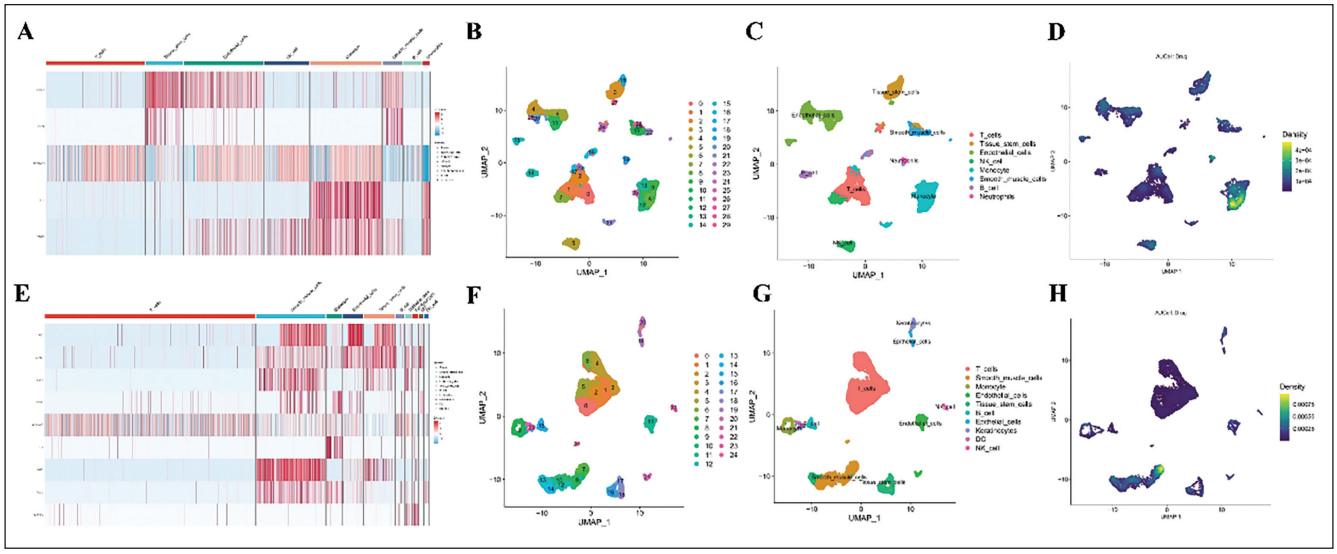


Figure 5. Cell Type Annotation and Hub Gene-Cell Relationships. (A) Hub Gene Expression Heatmap in Erosive Oral Lichen Planus (EOLP) Cell Types. (B) Unified Manifold Approximation and Projection (UMAP) Clustering of EOLP Cells (29 Clusters). (C) SingleR-based EOLP Cell Annotation. (D) The Distribution of Baicalein Target Cells in EOLP. (E) Hub Gene Expression Heatmap in Non-erosive Oral Lichen Planus (NEOLP) Cell Types. (F) UMAP Clustering of NEOLP Cells (24 Clusters). (G) SingleR-based NEOLP Cell Annotation. (H) The Distribution of Baicalein Target Cells in NEOLP.

delta T cells, plasmacytoid dendritic cells, memory B cells, and central memory CD8 T cells in OLP samples (Katou et al., 2007). Except for CD8 T cells, B cells may also play a greater role in the pathogenesis of OLP than expected (Orlandini et al., 2020). Baicalein possesses significant immunomodulatory effects, making it a potential therapeutic agent for autoimmune diseases (Xu et al., 2018). Researchers have reported that baicalein can mitigate immune dysfunction in sepsis by regulating the proportion of CD4+/CD8+T cells (Chen et al., 2022). Furthermore, baicalein has been shown to alleviate fibrosis and inflammation in systemic sclerosis by correcting B cell abnormalities (Peng et al., 2023). Thus, we believe that baicalein can also mitigate the immune disorder in OLP by regulating the function of CD8 cells and B cells.

Neutrophils could be annotated in EOLP samples, while epithelial cells, keratinocytes, and DC could be annotated in NEOLP samples. Neutrophil activation is a hallmark of inflammation (Craven et al., 2021). Neutrophil-mediated inflammation is implicated in the development of local erosions in OLP patients, as indicated by our results. Moreover, by utilizing the drug target AUCell function, we found that the hub genes of baicalein mainly acted on monocytes in the EOLP group. However, in the NEOLP group, the hub genes primarily targeted smooth muscle cells. Similar to neutrophils, monocytes also play a central role in inflammation, with monocytosis and monocyte activation being hallmark features of chronic inflammatory states (Knudsen et al., 2022). OLP is classified as a chronic inflammatory ailment. Studies have revealed that the expression level of TLR2 protein on monocytes in the OLP tissues is significantly higher than that in the healthy control tissues, which suggests the possibility of TLR2-mediated inflammatory activation of monocytes in OLP tissue (Ohno et al., 2011). The upregulation of IL-17 in the lesions of EOLP is more intensive compared with that of non-erosive reticular OLP. IL-17 can stimulate monocytes to produce IL-1 and TNF-α, thus amplifying the inflammatory response and leading to a more severe inflammation in EOLP tissue (Miossec, 2008). Hence, we postulate that the modulation of monocyte-mediated inflammation may be the primary mechanism by which baicalein treats EOLP. Given the limited number of smooth muscle cells in the oral cavity, it is unlikely that the therapeutic efficacy of baicalein in NEOLP involves smooth muscle cells (de Souza Fonseca et al., 2020).

Notwithstanding the insights our study provides into the therapeutic potential of baicalein for OLP, several limitations must be acknowledged. As a retrospective analysis utilizing existing datasets, our findings may be constrained by the relatively small sample size of the selected datasets and platform-specific biases inherent to dataset dependencies. Additionally, our study lacks both internal and external validation to further substantiate the reliability of our conclusions. Future research should prioritize well-designed *in vitro* and *in vivo* experiments to elucidate the molecular pathways modulated by baicalein, complemented by prospective clinical trials and validation across diverse patient cohorts to confirm therapeutic translatability.

Conclusion

A network pharmacology approach was employed in this study to examine the interactions and molecular mechanisms of baicalein in OLP. We examined 30 hub genes and three core targets (PTGS2, MMP2, and EGFR), which mediated the treatment effects of OLP with baicalein. From an immunoregulatory perspective, we hypothesized that baicalein may potentially ameliorate immune dysfunction in OLP patients by modulating CD8+T cells and B cells functionality. Analysis of single-cell sequencing data indicated that baicalein's therapeutic effect in EOLP involves modulating monocyte activation, and also implicated the estrogen and IL-17 signaling pathways in its mechanism of action for OLP. While these findings provide systematic theoretical support for baicalein's clinical potential, future studies must prioritize experimental validation and translational research to bridge computational predictions with clinical applicability. Our findings offer a systematic theoretical basis for justifying the clinical application of baicalein against OLP.

Abbreviations

AUC: Area under the curve; DEGs: Differentially expressed genes; EOLP: Erosive oral lichen planus; GEO: Gene expression omnibus; GO: Gene Ontology; KEGG: Kyoto Encyclopedia of Genes and Genomes; ME: Module feature genes; MCODE: Molecular complex detection; NEOLP: Non-erosive oral lichen planus; OLP: Oral lichen planus; PCA: Principal component analysis; PPI: Protein–protein interaction; ROC: Receiver operating characteristic; TOM: Topological overlap matrix; UMAP: Unified manifold approximation and projection; WGCNA: Weighted gene co-expression network analysis; GSEA: Gene set enrichment analysis.

Acknowledgments

The authors acknowledge the developers of all R packages utilized in their study. The authors acknowledge the "HOME for Researchers" for its help with the language of their manuscript.

Author Contributions

Chao Pei: Writing—review & editing. Dan Zhou and Zehan Zhang: Performed this study. Zhilin Chen and Jianxing Zhang: Provided suggestions. Dan Zhou and Zehan Zhang: Wrote the manuscript.

Data Availability

The data and materials can be acquired from SwissTargetPrediction database (https://www.swisstargetprediction.ch/), Comparative Toxicogenomics Database (CTD; https://ctdbase.org/), TargetNet database (https://targetnet.scbdd.com/), PharmMapper Server (http://www.lilab-ecust.cn/pharmmapper/), GEO database (https://www.ncbi.nlm.nih.gov/geo/) and our supplementary materials.

Declaration of Conflicting Interests

The authors declared no potential conflicts of interest with respect to the research, authorship, and/or publication of this article.

Ethical Approval and Informed Consent

This study neither required ethical approval nor consent to participate.

Funding

The authors received no financial support for the research, authorship, and/or publication of this article.

Supplementary Material

Supplementary material for this article is available online.

ORCID iD

Chao Pei https://orcid.org/0009-0003-7677-3990

References

Ahn, M. Y., Kang, J. K., Kwon, S. M., Yoon, H. E., & Yoon, J. H. (2020). Expression of nucleotide-binding oligomerization domain 1 and 2 in oral lichen planus. *Journal of Dental Sciences*, *15*(1), 1–8. https://doi.org/10.1016/j.jds.2019.12.005

Bao, J., Wu, Z., Zhang, C., Zhang, M., Wang, Y., Li, H., Sun, X., Gao, J., Ge, L., Li, Y., Wang, H., & Guo, Q. (2022). Efficacy and mechanism of osimertinib combined with bevacizumab in the treatment of postoperative EGFR positive stage II-IIIA lung adenocarcinoma. *American Journal of Translational Research*, *14*(1), 633–642.

Chen, H. Y., Zhang, S., Li, J., Huang, N., Sun, J., Li, B. H., Yang, J., & Li, Z. F. (2022). Baicalein attenuates severe polymicrobial sepsis via alleviating immune dysfunction of T lymphocytes and inflammation. *Chinese Journal of Integrative Medicine*, *28*(8), 711–718. https://doi.org/10.1007/s11655-022-3510-7

Chen, S. Y., Gao, Y., Sun, J. Y., Meng, X. L., Yang, D., Fan, L. H., Xiang, L., & Wang, P. (2020). Traditional Chinese Medicine: Role in reducing β-amyloid, apoptosis, autophagy, neuroinflammation, oxidative stress, and mitochondrial dysfunction of Alzheimer's disease. *Frontiers in Pharmacology*, *11*, 497. https://doi.org/10.3389/fphar.2020.00497

Choi, Y., Takasugi, M., Takemura, K., Yoshida, Y., Kamiya, T., Adachi, J., Tsuruta, D., & Ohtani, N. (2022). Characterization of transcriptomic and proteomic changes in the skin after chronic fluocinolone acetonide treatment. *Biomolecules*, *12*(12). https://doi.org/10.3390/biom12121822

Choi, Y. S., Baek, K., & Choi, Y. (2018). Estrogen reinforces barrier formation and protects against tumor necrosis factor alpha-induced barrier dysfunction in oral epithelial cells. *Journal of Periodontal & Implant Science*, *48*(5), 284–294. https://doi.org/10.5051/jpis.2018.48.5.284

Craven, T. H., Walton, T., Akram, A. R., Scholefield, E., McDonald, N., Marshall, A. D. L., Humphries, D. C., Mills, B., Campbell, T. A., Bruce, A., Mair, J., Dear, J. W., Newby, D. E., Hill, A. T., Walsh, T. S., Haslett, C., & Dhaliwal, K. (2021). Activated neutrophil fluorescent imaging technique for human lungs. *Scientific Reports*, *11*(1), 976. https://doi.org/10.1038/s41598-020-80083-w

de Souza Fonseca, R. R., Junior, M. A. R., Baruchi, D., Carvalho, T. R. B., Soares, A. B., de Menezes, S. A. F., de Jesus Viana

Pinheiro, J., & Fadul, J. N. F. (2020). Leiomyoma of the cheek. *Case Reports in Pathology*, *2020*, 8474905. https://doi.org/10.1155/2020/8474905

Ding, M., Wang, X., Wang, C., Liu, X., Zen, K., Wang, W., Zhang, C. Y., & Zhang, C. (2017). Distinct expression profile of HCMV encoded miRNAs in plasma from oral lichen planus patients. *Journal of Translational Medicine*, *15*(1), 133. https://doi.org/10.1186/s12967-017-1222-8

Fang, X., Wang, M., Zhou, X., Wang, H., Wang, H., & Xiao, H. (2022). Effects of growth years on ginsenoside biosynthesis of wild ginseng and cultivated ginseng. *BMC Genomics*, *23*(1), 325. https://doi.org/10.1186/s12864-022-08570-0

Gao, Z., Zhang, Y., Zhou, H., & Lv, J. (2020). Baicalein inhibits the growth of oral squamous cell carcinoma cells by downregulating the expression of transcription factor Sp1. *International Journal of Oncology*, *56*(1), 273–282. https://doi.org/10.3892/ijo.2019.4894

Gholizadeh, N., Sadeghi, A., Mirzaii-Dizgah, I., & Sheykhbahaei, N. (2021). Serum level of estrogen in Iranian patients with oral lichen planus. *Asian Biomedicine: Research, Reviews and News*, *15*(3), 145–150. https://doi.org/10.2478/abm-2021-0018

Guan, X., Shen, S., Liu, J., Song, H., Chang, J., Mao, X., Song, J., Zhang, L., & Liu, C. (2023). Protective effects of baicalin magnesium on non-alcoholic steatohepatitis rats are based on inhibiting NLRP3/Caspase-1/IL-1β signaling pathway. *BMC Complementary Medicine and Therapies*, *23*(1), 72. https://doi.org/10.1186/s12906-023-03903-2

Guillotin, D., Taylor, A. R., Platé, M., Mercer, P. F., Edwards, L. M., Haggart, R., Miele, G., McAnulty, R. J., Maher, T. M., Hynds, R. E., Jamal-Hanjani, M., Marshall, R. P., Fisher, A. J., Blanchard, A. D., & Chambers, R. C. (2021). Transcriptome analysis of IPF fibroblastic foci identifies key pathways involved in fibrogenesis. *Thorax*, *76*(1), 73–82. https://doi.org/10.1136/thoraxjnl-2020-214902

Gupta, A., Mohan, R. P., Gupta, S., Malik, S. S., Goel, S., & Kamarthi, N. (2017). Roles of serum uric acid, prolactin levels, and psychosocial factors in oral lichen planus. *Journal of Oral Science*, *59*(1), 139–146. https://doi.org/10.2334/josnusd.16-0219

He, B., Chen, Z., Nie, Y., Luo, M., Xu, S., Yan, J., & Chen, Z. (2022). Exploring and verifying the mechanism and targets of Shenqi pill in the treatment of nonalcoholic steatohepatitis via network pharmacology and experiments. *Journal of Immunology Research*, *2022*, 6588144. https://doi.org/10.1155/2022/6588144

Huang, L., Yu, Q., Peng, H., & Zhen, Z. (2023). The mechanism of peach kernel and safflower herb-pair for the treatment of liver fibrosis based on network pharmacology and molecular docking technology: A review. *Medicine (Baltimore)*, *102*(16), e33593. https://doi.org/10.1097/md.0000000000033593

Hyvärinen, E., Kashyap, B., & Kullaa, A. M. (2023). Oral sources of salivary metabolites. *Metabolites*, *13*(4), 498. https://doi.org/10.3390/metabo13040498

Katou, F., Ohtani, H., Watanabe, Y., Nakayama, T., Yoshie, O., & Hashimoto, K. (2007). Differing phenotypes between intraepithelial and stromal lymphocytes in early-stage tongue cancer. *Cancer Research*, *67*(23), 11195–11201. https://doi.org/10.1158/0008-5472.Can-07-2637

Knudsen, A. D., Bouazzi, R., Afzal, S., Gelpi, M., Benfield, T., Høgh, J., Thomsen, M. T., Trøseid, M., Nordestgaard, B. G., & Nielsen, S. D. (2022). Monocyte count and soluble markers of monocyte activation in people living with HIV and uninfected controls. *BMC Infectious Diseases*, *22*(1), 451. https://doi.org/10.1186/s12879-022-07450-y

Kumagai, K., Horikawa, T., Gotoh, A., Yamane, S., Yamada, H., Kobayashi, H., Hamada, Y., Suzuki, S., & Suzuki, R. (2010). Up-regulation of EGF receptor and its ligands, AREG, EREG, and HB-EGF in oral lichen planus. *Oral Surgery, Oral Medicine, Oral Pathology, Oral Radiology, and Endodontology*, *110*(6), 748–754. https://doi.org/10.1016/j.tripleo.2010.06.022

Lee, J. A., Shin, M. R., Park, H. J., & Roh, S. S. (2022). Scutellariae Radix and Citri Reticulatae Pericarpium mixture regulate PPARγ/RXR signaling in reflux esophagitis. *Evidence-Based Complementary and Alternative Medicine*, *2022*, 6969241. https://doi.org/10.1155/2022/6969241

Li, B., Lu, M., Jiang, X. X., Pan, M. X., Mao, J. W., & Chen, M. (2017). Inhibiting reactive oxygen species-dependent autophagy enhanced baicalein-induced apoptosis in oral squamous cell carcinoma. *Journal of Natural Medicines*, *71*(2), 433–441. https://doi.org/10.1007/s11418-017-1076-7

Li, H. B., Zhang, Y. H., Chen, H. Z., & Chen, Y. (2015). Expression of human DNA mismatch-repair protein, hMSH2, in patients with oral lichen planus. *Experimental and Therapeutic Medicine*, *9*(1), 203–206. https://doi.org/10.3892/etm.2014.2053

Li, S., & Zhang, B. (2013). Traditional Chinese medicine network pharmacology: Theory, methodology and application. *Chinese Journal of Natural Medicines*, *11*(2), 110–120. https://doi.org/10.1016/s1875-5364(13)60037-0

Li, Y., Wang, K., Zhang, B., Tu, Q., Yao, Y., Cui, B., Ren, B., He, J., Shen, X., Van Nostrand, J. D., Zhou, J., Shi, W., Xiao, L., Lu, C., & Zhou, X. (2019). Salivary mycobiome dysbiosis and its potential impact on bacteriome shifts and host immunity in oral lichen planus. *International Journal of Oral Science*, *11*(2), 13. https://doi.org/10.1038/s41368-019-0045-2

Liu, C., Li, Y., Chen, Y., Huang, S., Wang, X., Luo, S., Su, Y., Zhou, L., & Luo, X. (2020). Baicalein restores the balance of Th17/treg cells via aryl hydrocarbon receptor to attenuate colitis. *Mediators of Inflammation*, 2020, 5918587. https://doi.org/10.1155/2020/5918587

Markowski, A., Zaremba-Czogalla, M., Jaromin, A., Olczak, E., Zygmunt, A., Etezadi, H., Boyd, B. J., & Gubernator, J. (2023). Novel liposomal formulation of baicalein for the treatment of pancreatic ductal adenocarcinoma: Design, characterization, and evaluation. *Pharmaceutics*, *15*(1). https://doi.org/10.3390/pharmaceutics15010179

Miossec, P. (2008). Dynamic interactions between T cells and dendritic cells and their derived cytokines/chemokines in the rheumatoid synovium. *Arthritis Research & Therapy*, *10*(Suppl. 1), S2. https://doi.org/10.1186/ar2413

Nicolae, I., Mitran, C. I., Mitran, M. I., Ene, C. D., Tampa, M., & Georgescu, S. R. (2017). Ascorbic acid deficiency in patients with lichen planus. *Journal of Immunoassay and Immunochemistry*, *38*(4), 430–437. https://doi.org/10.1080/15321819.2017.1319863

Ohno, S., Tateishi, Y., Tatemoto, Y., Morishita, K., Sasabe, E., & Yamamoto, T. (2011). Enhanced expression of toll-like receptor 2 in lesional tissues and peripheral blood monocytes of patients with oral lichen planus. *Journal of Dermatology*, *38*(4), 335–344. https://doi.org/10.1111/j.1346-8138.2010.00956.x

Orlandini, R., Jacinto, R., Teixeira, L. R., Silva, G. A., Gallo, C. B., Innocentini, L., Ribeiro-Silva, A., & Motta, A. C. F. (2020). Evidence for a significant role of B-cells in the pathogenesis of

oral lichen planus: Preliminary results of a cross-sectional study. *Journal of Cutaneous Pathology*, *47*(3), 310–313. https://doi.org/10.1111/cup.13636

Park, S. Y., Lee, H. J., Kim, S. H., Kim, S. B., Choi, Y. H., Kim, Y. K., & Yun, P. Y. (2018). Factors affecting treatment outcomes in patients with oral lichen planus lesions: A retrospective study of 113 cases. *Journal of Periodontal & Implant Science*, *48*(4), 213–223. https://doi.org/10.5051/jpis.2018.48.4.213

Peng, B., Hu, Q., He, R., Hou, H., Lian, D., Chen, Y., Li, H., Song, L., Gao, Y., Chen, T., Zhang, G., & Li, J. (2023). Baicalein alleviates fibrosis and inflammation in systemic sclerosis by regulating B-cell abnormalities. *BMC Complementary Medicine and Therapies*, *23*(1), 62. https://doi.org/10.1186/s12906-023-03885-1

Peng, Q., Zhang, J., Ye, X., & Zhou, G. (2017). Tumor-like microenvironment in oral lichen planus: Evidence of malignant transformation? *Expert Review of Clinical Immunology*, *13*(6), 635–643. https://doi.org/10.1080/1744666x.2017.1295852

Pouralibaba, F., Babaloo, Z., Pakdel, F., & Aghazadeh, M. (2013). Serum level of interleukin 17 in patients with erosive and non erosive oral lichen planus. *Journal of Dental Research, Dental Clinics, Dental Prospects*, *7*(2), 91–94. https://doi.org/10.5681/joddd.2013.016

Rankin, L., Gouveia-Figueira, S., Danielsson, K. P., & Fowler, C. J. (2020). Relative deficiency of anti-inflammatory *n*-acylethanolamines compared to prostaglandins in oral lichen planus. *Biomedicines*, *8*(11), 481. https://doi.org/10.3390/biomedicines8110481

Sperandio, M., Klinikowski, M. F., Brown, A. L., Shirlaw, P. J., Challacombe, S. J., Morgan, P. R., Warnakulasuriya, S., & Odell, E. W. (2016). Image-based DNA ploidy analysis aids prediction of malignant transformation in oral lichen planus. *Oral Surgery, Oral Medicine, Oral Pathology and Oral Radiology*, *121*(6), 643–650. https://doi.org/10.1016/j.oooo.2016.02.008

The UniProt Consortium. (2018). UniProt: The universal protein knowledgebase. *Nucleic Acids Research*, *46*(5), 2699. https://doi.org/10.1093/nar/gky092

Wang, J., Luo, H., Xiao, Y., & Wang, L. (2016). miR-125b inhibits keratinocyte proliferation and promotes keratinocyte apoptosis in oral lichen planus by targeting MMP-2 expression through PI3K/Akt/mTOR pathway. *Biomedicine & Pharmacotherapy*, *80*, 373–380. https://doi.org/10.1016/j.biopha.2016.02.043

Xu, J., Liu, J., Yue, G., Sun, M., Li, J., Xiu, X., & Gao, Z. (2018). Therapeutic effect of the natural compounds baicalein and baicalin on autoimmune diseases. *Molecular Medicine Reports*, *18*(1), 1149–1154. https://doi.org/10.3892/mmr.2018.9054

Yang, M., Xu, J., Zhang, F., Luo, P., Xu, K., Feng, R., & Xu, P. (2023). Large-scale genetic correlation analysis between spondyloarthritis and human blood metabolites. *Journal of Clinical Medicine*, *12*(3), 1201. https://doi.org/10.3390/jcm12031201

Zhao, S., Mo, X., Wen, Z., Ren, L., Chen, Z., Lin, W., Wang, Q., Min, S., & Chen, B. (2022). Comprehensive bioinformatics analysis reveals the hub genes and pathways associated with multiple myeloma. *Hematology*, *27*(1), 280–292. https://doi.org/10.1080/16078454.2022.2040123

Zheng, Z., Chen, J., Chen, X., Huang, L., Xie, W., Lin, Q., Li, X., & Wong, K. C. (2023). Enabling single-cell drug response annotations from bulk RNA-Seq using SCAD. *Advanced Science (Weinh)*, *10*(11), e2204113. https://doi.org/10.1002/advs.202204113

Zhong, E. F., Chang, A., Stucky, A., Chen, X., Mundluru, T., Khalifeh, M., & Sedghizadeh, P. P. (2020). Genomic analysis of oral lichen planus and related oral microbiome pathogens. *Pathogens*, *9*(11), 952. https://doi.org/10.3390/pathogens9110952